Formation of chlorobenzenes by oxidative thermal decomposition of 1,3-dichloropropene

Nwakamma Ahubelem[a], Kalpit Shah[a], Behdad Moghtaderi[a], Mohammednoor Altarawneh[b], Bogdan Z. Dlugogorski[b], , Alister J. Page[a]

[a] Newcastle Institute for Energy and Resources, The University of Newcastle, Callaghan, NSW 2308, Australia

[b] School of Engineering and Information Technology Murdoch University, Murdoch, WA 6150, Australia

Abstract

We combine combustion experiments and density functional theory (DFT) calculations to investigate the formation of chlorobenzenes from oxidative thermal decomposition of 1,3-dichloropropene. Mono- to hexa-chlorobenzenes are observed between 800 and 1150 K, and the extent of chlorination was proportional to the combustion temperature. Higher chlorinated congeners of chlorobenzene (tetra-, penta-, hexa-chlorobenzene) are only observed in trace amounts between 950 and 1050 K. DFT calculations indicate that cyclisation of chlorinated hexatrienes proceeds via open-shell radical pathways. These species represent key components in the formation mechanism of chlorinated polyaromatic hydrocarbons. Results presented herein should provide better understanding of the evolution of soot from combustion/pyrolysis of short chlorinated alkenes.

Keywords: 1,3-Dichloropropene; Chlorobenzene; Cyclisation; Density functional theory; Combustion

Introduction

1,3-Dichloropropene (1,3-D) is used extensively in agriculture as a pre-plant soil-fumigant primarily for the control of parasites and soil-borne bacteria and viruses. 1,3-D was first introduced in 1956 and is now widely used in many countries, including the USA, Canada, Australia and the European Union (where it is currently being phased out). The extensive use of pesticides has stimulated research aimed at understanding the chemical mechanism and products of their combustion [1-3]. These products can include highly toxic species, such as dioxins and their precursors. While a number of investigations have focused on toxicity of 1,3-D [4-6], the mechanism(s) and products of its combustion have not yet been reported.

Thermal decomposition of chlorinated alkanes and alkenes typically results in chlorinated aromatic pollutants. Precursors of polychlorinated dibenzo-*p*-dioxins and dibenzofurans (PCDD/F) have been observed during the heterogeneous oxidative/pyrolytic decomposition of chloroaliphatic hydrocarbons [7]. Similarly, chloroaromatic compounds and their precursors have been detected during the decomposition of chlorinated short-chain aliphatic hydrocarbons [7-23]. The latter investigations show that formation of PCDD/F precursors proceeds *via* molecular growth reactions triggered by alkyl and chlorinated vinyl radicals [16,21,22]*via* rearrangement and radical recombination between unsaturated intermediates [9].

Benzene and chlorobenzenes have also been identified and quantified in the combustion of chlorinated short-chain hydrocarbons [15,23]. The formation of these chloroaromatic compounds has been attributed to *de novo* processes enabled by soot particles in the flame in addition to coupling of gas phase precursors. High yields of hexachlorobenzene were observed during fly ash-catalysed combustion of trichloroethylene [12]. This supports the theory that chloroaromatic compounds can be formed in the high-temperature post combustion zone, which provides the precursors necessary for PCDD/F formation in lower temperature zones. Similarly, hexachlorobenzene was observed during the pyrolysis of hexachloropropene above 773 K, *via* self-recombination of C_3Cl_5 radicals [19]. These radicals are produced during the initial decomposition of hexachloropropene (C_3Cl_6). It is also

possible for chlorine atoms to recombine with propene or any available radical to form the trichloropropargyl radical, which can self-recombine to produce chlorinated benzenes. Pyrolysis of trichloroethene above 1000 K has also been observed to yield hexachlorobenzene [21].

In this work, we investigate formation of chlorobenzenes, *via* high-temperature combustion of 1,3-D using a combined experimental and quantum chemical approach. Chlorobenzenes have been categorised by the International Agency for Research on Cancer (IARC) as a Group 2B animal carcinogen and a potential human carcinogen, and in addition they are precursors of PCDD/Fs [8,17,18]. Experiments show that between 650 and 1050 K, combustion products of 1,3-D include mono- to hexa-chlorinated benzenes. Quantum chemical calculations of reaction pathways reveal that these products can form via a number of alternate cyclisation pathways. The most thermodynamically and kinetically favourable pathways are observed to be propagated by perchlorohexatriene-derived radicals. Kinetic and thermodynamic parameters presented here will be useful for future kinetic models of halohydrocarbon combustion. Formation of the first chlorinated aromatic ring typically initiates the formation of chlorinated polyaromatic hydrocarbons (PAHs). Results from this study will also contribute toward a better understanding of the formation of soot during combustion of chlorinated short-chain hydrocarbons.

Methods

Experimental

The experimental apparatus employed in the thermal decomposition of 1,3-D is illustrated in Fig. 1.

1,3-D (98%, Dow Agroscience, Australia), a faint yellow liquid at room temperature, was introduced into the system using a syringe pump operated at a constant rate to keep the reactant concentration at 8580 ppm, in a dilute stream of air in nitrogen (6% O_2). We used a heating tape (set at 403 K) to ensure proper vaporisation of the reactant prior to entering the reactor and also minimise temperature gradients inside the reactor. The resulting vapour/nitrogen mixture entrained a controlled amount of

oxygen, with oxygen concentration monitored on the molecular sieve channel 1 of a 490 micro gas chromatograph (Agilent, USA). We used the molecular sieve and Poraplot Q columns of the same micro GC to measure the CO and CO_2 produced during the experiment with the micro GC calibrated with a gas standard. The chloride ion obtained from NaOH trap was analysed using Dionex DX-100 ion chromatograph. We used drierite to remove the water vapour prior to product analyses in order to avoid damage to our analytic instruments.

The jet stirred reactor (JSR) used here consists of a sphere (54 mm i.d., 82.3 cm^3 in volume), made of quartz (99.99% purity to minimise wall catalytic reactions). The spherical part of the reactor is equipped with four nozzles each of 3 mm i.d. for the injection of the feed gas and reactant vapour thereby obtaining the stirring. The reactor is aligned along the centreline of an electrically heated single-zone furnace (Brother furnace China) calibrated from 623 K to 1123 K with a thermocouple placed along the tube to define a uniform temperature zone. The tail end of the reactor was connected to different product collection systems.

Once the temperature and reactor conditions are stabilised, reactants are introduced into the reactor via the syringe pump at a steady state and product sampling from the reactor commences immediately. The experiments were carried out over a wide temperature range of 673–1073 K with an equivalence ratio of 0.5. For all experiments, the pressure was 1 atm and the residence time was 10 s. Sampling of reactants, stable intermediates and products from the reactor lasted for 3 h in each run. The polytetrafluoroethylene connection tubes are normally rinsed with dichloromethane and/or hexane solution to recover adsorbed products and to avoid contamination of succeeding runs. We used a glass tube loaded with 200 mg of XAD-2 resin (Supelpak-2, Sigma–Aldrich, Australia) and connected it at the reactor outlet as our VOC trap. Hexane and dichloromethane (DCM) solvent trap was chilled in a cold glycol bath (273 K) to collect any condensable products.

Products were analysed with GC–MS. We adapted the general procedures of the National Institute for Occupational Safety and Health (NIOSH) method 1003. We used XAD-2 resin (in place of activated charcoal) as the adsorbent and *n*-hexane (instead of CS_2) as the solvent. After each experiment, the

used XAD-2 resin was collected and sonicated with 40 mL hexane for 2 h. The XAD-2 extract was filtered and injected (split ratio 10:1) into the Agilent 7890 GC and 7200 Accurate-mass Q-TOF GC/MS with a 30 m Agilent HP-5MS column (i.d. of 250 μm and film thickness of 0.25 μm). In addition, we combined the solvent from washing the reactor tube together with solution from the solvent trap and then injected at a split ratio of 10:1 into the same GC–MS with the same operating conditions. The GC–MS carrier gas (helium) flowed at a constant rate of 1.2 mL/min and pressure of 9.8 psi. The injector temperature was maintained at 513 K and the injection volume was 1 μL. The GC oven temperature commenced at 323 K, and then held for 1 min and then ramped at 283 K per minute to 573 K and held for 1 min. We maintained the transfer line temperature at 513 K. The MS electron impact energy was set at 70 eV and the emission current was maintained at 2.8 μA with an ion source of 503 K. We identified the product species on the basis of NIST library searches, examination of mass spectra (the ratio of Cl element, loss of characteristic fragments and molecular ions), authentic standard injection and standard elution order. The quantitation of the VOCs relied on the preparation of external standard calibration curves.

Computational methods

Reaction pathways were investigated using density functional theory (DFT) with Truhlar's (U)M06-2X functional [24,25], in conjunction with a 6-311+G(d,p) basis set. Mardirossian and Head-Gordon [26] have recently shown that M06-2X provides good overall performance for reaction thermochemistry. Nevertheless, to ensure this is the case in the current context, we compare M06-2X-calculated kinetic and thermodynamic parameters with G3MP2B3 [27] and experimental values (see Tables S1 and S2 in the Supporting Information). G3MP2B3 has previously been shown to provide accurate reaction thermochemistry for typical combustion reactions [28]. The structures of all reaction intermediates and transition states (TSs) were optimised using Gaussian 09 [29]; all TSs were verified by having one negative harmonic vibrational frequency. The intrinsic reaction coordinate (IRC) method [30] was used to ensure that each TS corresponded to the correct reactive pathway. The Chemrate code [31] facilitated the computation of kinetic parameters based on calculated vibrational

frequencies and rotational constants. Unless stated otherwise, enthalpic contributions were calculated at 298.15 K.

Results and discussion

Thermal decomposition of 1,3-dichloropropene

1,3-D exhibited only minimal degradation at temperatures <673 K, with combustion initiating at *ca*. 673 K (Fig. 2). At 823 K, approximately half of the 1,3-D is consumed, and this increases dramatically to >90% by 873 K. At higher temperatures, effectively all 1,3-D is consumed by the combustion process.

Fig. 2 ; Fig. 3 show the yields of mono- to hexa-chlobenzenes obtained from oxidative decomposition of 1,3-D between 650 and 1050 K. The main products of the thermolysis of 1,3-D were CO, CO2 and HCl, which accounted for up to ~90% of product yield depending on the experimental condition (see Supporting Information, Table S4). Water vapour was also observed as a major product, but was not quantified. Of the minor products, mono to hexachlorobenzenes were produced in greatest abundance, constituting up to 0.6% of product yield, depending on reaction temperature. Other minor products obtained included hexachlorobutadiene, hexachloroethane, 2-chloronaphthalene, dibenzofuran, ethenylbenzofuran, chlorindanon and chloronaphthalenol (see Supporting Information, Tables S4 and S5, Figs. S8 and S9).

Since decomposition of 1,3-D was carried out in an oxidative environment, oxygenated species (i.e. in ketone and enol derivatives) may have formed but were not detected. This could be because our detection system has been optimised for heavier chlorinated molecules, such as polychlorinated dibenzo-*p*-dioxins and polychlorinated dibenzofurans, using adsorption of these species on the XAD-2 resin. HCl formation mechanisms, and their relation to the formation of chlorobenzenes, are discussed in greater detail below. The formation of CO_2, CO and H_2O from combustion of small saturated and unsaturated hydrocarbons has already been studied on a number of

occasions [32,33,34]. These reactions are initiated by hydrogen abstraction by O_2, forming HO_2 radicals. Hydrogen abstractions by HO_2 produces H_2O_2 which readily dissociates into OH radicals at higher temperatures. As a result, at temperatures <800 K, OH is expected to be the main reaction carrier [33]. It follows that the manner in which 1,3-D decomposition is initiated is temperature dependent. Subsequent reactions are then driven by HO_2 and OH radicals [32,33]. H_2O is formed directly by OH-mediated hydrogen abstraction, whereas CO and CO_2 are formed primarily from reaction between aldehyde radicals and O_2. HO_2 and OH radicals also drive the formation of CO_2 by the direct oxidation of CO. Table S3 shows that the yield of CO_2 was proportional to the reaction temperature between 673 and 1073 K. On the other hand, CO yield peaked at 973 K, decreasing at higher temperatures (Table S3). This indicates that temperature dependent mechanisms are responsible for CO_2 formation, consistent with a previous study [33].

Production of chlorobenzenes (i.e. minor products) is observed at 773 K and above, with the highest yield occurring at 823 K for chlorobenzene and 923 K for dichlorobenzene. We note here that there is little selectivity between 1,3- and 1,4-dichlorobenzene, while the yield of 1,2-dichlorobenzene is *ca*. 10% higher by comparison. Trichlorobenzenes were produced at 923 K and above (Fig. 3). The maximum yield of 1,3,5-trichlorobenzene, *ca*. 65% of minor products (obtained at 923 K), was far greater than either 1,2,3-trichlorobenzene and 1,2,4-trichlorobenzene, which peaked at *ca*. 10% of minor products (between 923 and 1023 K). This can be understood in terms of steric/electrostatic repulsion between individual Cl atoms on the benzene ring, and is consistent with the relative thermodynamic stabilities of these three isomers calculated using G3MP2B3 (not shown). At temperatures higher than 1023 K, di- and tri-chlorobenzenes were not observed. Figure 3 shows that higher temperatures favoured the production of tetra- to hexa-chlorobenzenes. Of these, pentachlorobenzene was produced with the greatest yield (40% of minor products at 973 K), followed by 1,2,3,4-tetrachlorobenzene (20% of minor products at 973 K). This suggests that pentachlorobenzene may form from further chlorination of 1,2,3,4-tetrachlorobenzene and hence the latter plays a more active role as a reactive intermediate during combustion, compared to pentachlorobenzene (which is more of a reactive “sink”). The alternative tetrachlorobenzene isomer

was not observed here. Hexachlorobenzene was also observed in this temperature range, however at relatively low levels (maximum yield was <10% of minor products at 973 K).

Reaction initiation

Thermal decomposition of hexachloropropene [19] and propene [35,36] can be initiated by unimolecular processes (bond scission) and bimolecular processes involving O_2. It is likely that similar processes and kinetics control the initial stages of 1,3-D thermal decomposition studied here. For propene, the kinetic data for O_2 abstraction of the allylic hydrogen atom, forming HO_2 and a propene-derived radical have been estimated previously [35,36]. Hexachloropropene has been shown to undergo unimolecular C–Cl bond scission at elevated temperatures, comparable to those used in this work. Kinetic parameters for the latter process are more favourable; C–Cl bond scission corresponds to an Arrhenius prefactor (A) and activation energy (E_a) of 5.0×10^{16} s^{-1} and 236.6 kJ/mol, respectively for a temperature range of (573–773 K) [19]. On the other hand, for H-abstraction from the allylic site of propene by O_2, $A = 1 \times 10^{-10}$ cm^3 mol^{-1} $s^{-1}$and E_a = 199.1 kJ/mol between 300 and 2500 K [36]. Under lean oxidation conditions relevant to this study, scission of C–Cl bonds is expected to hold more importance as an initiation channel, if compared with the O_2-mediated pathway. C–Cl bond scission of 1,3-D forming 1,3-D-derived radical species is therefore a plausible activation step in 1,3-D thermal decomposition. DFT and G3MP2B3 calculations corroborate this assumption (see Supporting Information).

Alternatively, HO_2 and OH radicals can initiate the formation of chlorobenzenes, via radical abstraction of Cl from either vinyllic or allylic sites of 1,3-D. Scheme S3 shows that these processes are thermodynamically competitive with C–Cl bond scission processes. This is because the Cl–OH bond is ∼100 kJ/mol more stable, compared to the Cl–OOH bond, which stabilises the product more in the case of OH-mediated abstraction. This is in agreement with the findings of Wilk et al. [33], who showed that OH abstracting H from propene was found to be a more dominant reaction than HO_2 abstraction reactions.

A number of previous investigations have shown that small aromatic molecules can form via cyclisation of unsaturated hydrocarbons (e.g., 1,3,5-hexatriene [28], hexachloropropene [19-37]). Here we investigate if this is also potentially the case for chlorobenzenes. Chlorobenzene can conceivably form via cyclisation of the 1,6-dichlorohexatriene precursor (IM4), which is observed in appreciable amounts in our combustion experiments (see Supporting Information). During combustion, there are undoubtedly chemical reactions including chemical pathways to IM4 and subsequently chlorobenzene. We postulate that, radical recombination reactions, beginning with 1,3-D-derived radical (IM1), are prominent amongst these. Self-recombination of IM1 (Scheme 1(a)) produces 1,6-dichlorohexadiene (IM2) and is exothermic ($\Delta_r H^o_{298}$ = −210.5 kJ/mol). Subsequent dehydrogenation of IM2 at either allylic carbon via Cl is also exothermic ($\Delta_r H^o_{298}$ = −67.2 kJ/mol) and results in the 1,6-dichlorohexadiene radical IM3. Abstraction of hydrogen from the remaining allylic carbon by Cl ($\Delta_r H^o_{298}$ = −232.3 kJ/mol) results in the formation of the cyclisation precursor IM4. M06-2X/6-311+G(d,p) calculations show that both of the abstractions are barrierless, as anticipated.

Chlorobenzene formation

Closed-shell cyclisation of 1,6-dichlorohexatriene (forming chlorobenzene) and octachlorohexatriene (forming hexachlorobenzene) are unlikely on a kinetic basis (see Supporting Information). Under our reaction conditions, it is far more likely that radical cyclisation is responsible for chlorobenzene formation, as proposed by Hudson et al. [38]. In the case of chlorobenzenes, radical cyclisation would necessitate the scission of either a C–Cl or C–H bond in 1,2-dichlorohexatriene, and as noted above, the former is the more likely pathway (based on the results for 1,3-D, see Supporting Information). As for 1,3-D, an alternative to bond scission here is Cl/H abstraction by ambient Cl. $\Delta_r H^o_{298}$and $\Delta H^{\ddagger}$ for this process in 1,6-dichlorohexatriene are similar to those for 1,3-D (Scheme 2(a)). However, abstraction of H by Cl at the C(3) carbon (Scheme 2(b)) is substantially more favourable, with $\Delta H^{\ddagger}$ = 104 kJ/mol and $\Delta_r H^o_{298}$ = 96.3 kJ/mol. H/Cl abstraction by H atoms is also possible, (Scheme 2(c) and (d)), and follow the same kinetic trend as abstraction with Cl. For instance, H abstraction at the terminal position has an activation enthalpy of 90.7 kJ/mol, whereas abstraction at C(3) is only

45.8 kJ/mol. The thermodynamics of Cl abstraction by H, or H abstraction by Cl, are consistent with the higher bond enthalpy in HCl as opposed to Cl_2.

The PES for cyclisation of 1,6-dichlorohexatriene-derived radical IM5 is shown in Fig. 4. The most prohibitive step of this pathway is the initial rotation around the C(3)–C(4) bond, which has an activation enthalpy of 159.5 kJ/mol. The rate constant *k* for this step (IM5 → IM7) at 873 K is calculated to be 445.5 s^{-1} (see Table S1 for further kinetic parameters). All subsequent steps in this mechanism are considerably more labile. Rotations around the C(2)–C(3) bond (IM7 → IM8) and C(4)–C(5) bond (IM8 → IM9) require only 32.5 and 44.1 kJ/mol, respectively. IM9 undergoes ring closure to form the chlorocyclohexadiene-derived radical IM10. The latter step is highly exothermic ($\Delta_r H^o_{298}$ = −239.3 kJ/mol) with a barrier of 33.4 kJ/mol. Formation of chlorobenzene from IM10 can occur *via* H abstraction with Cl; this process is effectively barrierless and is exothermic by −278.7 kJ/mol. In addition to unimolecular elimination of HCl from the parent 1,3-D molecule and possibly other chlorinated species [37], bimolecular abstraction reactions (i.e. reactions b and d in Scheme 2) constitute major pathways for the formation of HCl.

As opposed to the cyclisation of IM5, the cyclisation of IM6 represents a more favourable reaction pathway (Fig. 5). The initial rotation about the C(2)–C(3) bond passes through an isoenergetic TS before forming IM11 ($\Delta_r H^o_{298}$ = −33.3 kJ/mol). The two subsequent bond rotations that result in IM13 have barriers less than 30 kJ/mol. Ultimately the rate-limiting step in this reaction pathway is ring closure (IM13 → IM14), which has a barrier of 140.3 kJ/mol. Kinetic parameters for this final ring-closure step are included in Table S1.

IM14 can subsequently undergo H addition at C(3), which is highly exothermic ($\Delta_r H^o_{298}$ = −475.3 kJ/mol) and barrierless (Fig. 6(a)). The formed dichlorocyclohexadiene (IM15) can lead to chlorobenzene *via* unimolecular HCl elimination with an activation enthalpy of 115.8 kJ/mol and reaction enthalpy of −92.5 kJ/mol (Fig. 6(b)).

Generally, the results from M06-2X/6-311+G(d,p) and G3MP2B3 calculations are similar except for the reactions 2IM1 → IM2 (Scheme 1(a)), IM10 + Cl → P1 (Fig. 4), IM13 → IM14 (Fig. 5) and TS14 (Fig. 6). In our M06-2X calculations, we have optimised geometries and calculated vibrational frequencies using M06-2X/6-311+G(d,p). However, G3MP2B3 method uses optimized structural geometries, vibrational frequencies and zero point energies calculated with B3LYP/6-31G(d). We found no significant variance in the optimized geometries, vibrational frequencies and zero point energies using the two different methods. The deviations between M06-2X and G3MP2B3 results could be attributable to an improved single point energy results of G3MP2B3 using MP2(FC)/G3MP2large

Conclusions

The formation of chlorobenzenes *via* oxidative thermal decomposition of 1,3-D has been investigated with a combined experimental and computational approach. Yields of mono- and dichlorobenzenes are highest between 800 and 950 K, while higher temperatures can lead to tri- to hexa-chlorobenzenes at significantly lower yields. Theoretical calculations have revealed that radical-derived propagation (i.e. open shell pathway) plays a potentially major role in the formation of mono and dichlorobenzenes. Cyclisation of 1,3-D derived molecular precursors is associated with prohibitively high kinetic barriers. On the other hand, H-abstraction at both allylic and vinylic sites in these precursors leads to kinetically more competitive reaction pathways.

Acknowledgments

This study was supported by Australian Research Council (ARC) Discovery Project funding and supercomputing grants from The National Computational Infrastructure (NCI) National Facility and INTERSECT. N.A. thanks The University of Newcastle for a postgraduate research scholarship and Prof. Keiji Morokuma (Kyoto University) for useful discussions.

References

[1] R. Nageswara Rao, S. Khalid, T. Rajani, S. Husain, J. Chromatogr. A 954 (1–2) (2002) 227–234.

[2] O. Senneca, F. Scherillo, A. Nunziata, J. Anal. Appl. Pyrol. 80 (1) (2007) 61–76.

[3] J. Vikelsøe, E. Johansen, Chemosphere 40 (2) (2000) 165–175.

[4] P. Flessel, J. Golsmith, E. Kahn et al., Acute and Possible Long Term Effects of 1,3-Dichloropropene, 1978, Report (CDC) 78–8017.

[5] T. Clary, B. Ritz, Am. J. Ind. Med. 43 (3) (2003) 306–313.

[6] S. Cracknel, G. Jackson, C. Hardy, 1,3-Dichloropropene-Acute Inhalation Study in Rats-4 hour Exposure, 1987, NTIS Report 86-870002297.

[7] K.L. Froese, O. Hutzinger, Environ. Sci. Technol. 30 (3) (1996) 998–1008

[8] M. Altarawneh, B.Z. Dlugogorski, E.M. Kennedy, J.C. Mackie, Prog. Energy Combust. Sci. 35 (3) (2009) 245–274.

[9] W.D. Chang, S.M. Senkan, Symp. (Int.) Combust. 22 (1) (1989) 1453–1459.

10] W.D. Chang, S.M. Senkan, Environ. Sci. Technol. 23 (4) (1989) 442–450.

[11] G. Eklund, J.R. Pedersen, B. Strömberg, Chemosphere 16 (1) (1987) 161–166.

[12] K.L. Froese, O. Hutzinger, Chemosphere 28 (11) (1994) 1977–1987.

[13] K.L. Froese, O. Hutzinger, Environ. Sci. Technol. 30 (3) (1996) 1009–1013.

[14] K.L. Froese, O. Hutzinger, Environ. Sci. Technol. 31 (2) (1997) 542–547.

[15] M. Kassem, S.M. Senkan, Combust. Flame 83 (3–4) (1991) 365–374.

[16] D. Lenoir, A. Wehrmeier, K.-W. Schramm, A. Kaune, R. Zimmermann, P.H. Taylor, S.S. Sidhu, Environ. Eng. Sci. 15 (1) (1998) 37–47.

[17] P. Mulder, J. Warieja, Organohalogen Compd. 11 (1993) 273–276.

[18] P.M. Sommeling, P. Mulder, R. Louw, Chemosphere 29 (9) (1994) 2015–2018.

[19] P.H. Taylor, D.A. Tirey, B. Dellinger, Combust. Flame 105 (4) (1996) 486–498.

[20] P.H. Taylor, D.A. Tirey, B. Dellinger, Combust. Flame 106 (1–2) (1996) 1–10.

[21] P.H. Taylor, D.A. Tirey, W.A. Rubey, B. Dellinger, Combust. Sci. Technol. 101 (1– 6) (1994) 75–102.

[22] A. Wehrmeier, D. Lenoir, S.S. Sidhu, P.H. Taylor, W.A. Rubey, A. Kettrup, B. Dellinger, Environ. Sci. Technol. 32 (18) (1998) 2741–2748.

[23] M. Xieqi, B. Cicek, S.M. Senkan, Combust. Flame 94 (1–2) (1993) 131–145.

[24] B.J. Lynch, D.G. Truhlar, J. Phys. Chem. A 105 (13) (2001) 2936–2941.

[25] Y. Zhao, D.G. Truhlar, Chem. Phys. Lett. 502 (1–3) (2011) 1–13.

[26] N. Mardirossian, M. Head-Gordon, Phys. Chem. Chem. Phys. 16 (21) (2014) 9904–9924.

[27] A.G. Baboul, L.A. Curtiss, P.C. Redfern, K. Raghavachari, J. Chem. Phys. 110 (16) (1999) 7650.

[28] H. Detert, D. Lenoir, H. Zipse, Eur. J. Org. Chem. 2009 (8) (2009) 1181–1190.

[29] Gaussian 09, Revision D.01, M.J. Frisch, G.W. Trucks, H.B. Schlegel, G.E. Scuseria, M.A. Robb, J.R. Cheeseman, G. Scalmani, V. Barone, B. Mennucci, G.A. Petersson, H. Nakatsuji, M. Caricato, X. Li, H.P. Hratchian, A.F. Izmaylov, J. Bloino, G. Zheng, J.L. Sonnenberg, M. Hada, M. Ehara, K. Toyota, R. Fukuda, J. Hasegawa, M. Ishida, T. Nakajima, Y. Honda, O. Kitao, H. Nakai, T. Vreven, J.A. Montgomery, Jr., J.E. Peralta, F. Ogliaro, M. Bearpark, J.J. Heyd, E. Brothers, K.N. Kudin, V.N. Staroverov, R. Kobayashi, J. Normand, K. Raghavachari, A. Rendell, J.C. Burant, S.S. Iyengar, J. Tomasi, M. Cossi, N. Rega, J.M. Millam, M. Klene, J.E. Knox, J.B. Cross, V. Bakken, C. Adamo, J. Jaramillo, R. Gomperts, R.E. Stratmann, O. Yazyev, A.J. Austin, R. Cammi, C. Pomelli, J.W. Ochterski, R.L. Martin, K. Morokuma, V.G. Zakrzewski, G.A. Voth, P. Salvador, J.J. Dannenberg, S. Dapprich, A.D. Daniels, Ö. Farkas, J.B. Foresman, J.V. Ortiz, J. Cioslowski, D.J. Fox, Gaussian, Inc., Wallingford CT, 2009.

[30] K. Fukui, Acc. Chem. Res. 14 (12) (1981) 363–368.

[31] V. Mokrushin, V. Bedanov, W. Tsang, M. Zachariah, V. Knyazev, NIST, Gaithersburg, MD, 2002.

[32] K. Chenoweth, A.C. van Duin, W.A. Goddard, J. Phys. Chem. A 112 (5) (2008) 1040–1053.

[33] R.D. Wilk, N.P. Cernansky, W.J. Pitz, C.K. Westbrook, Combust. Flame 77 (2) (1989) 145–170.

[34] A.J. Page, B. Moghtaderi, J. Phys. Chem. A 113 (8) (2009) 1539–1547.

[35] D. Baulch, C. Cobos, R. Cox, C. Esser, P. Frank, T. Just, J. Kerr, M. Pilling, J. Troe, R. Walker, J. Phys. Chem. Ref. Data 21 (3) (1992) 411–734.

[36] W. Tsang, J. Phys. Chem. Ref. Data 20 (2) (1991) 221–273.

[37] N. Ahubelem, M. Altarawneh, B.Z. Dlugogorski, Organohalogen Compd. 74 (2012) 640–643.

[38] C.E. Hudson, D.J. McAdoo, J. Am. Soc. Mass Spectrom. 18 (2) (2007) 270–278.

Fig. 1. Schematic of the experimental set-up.

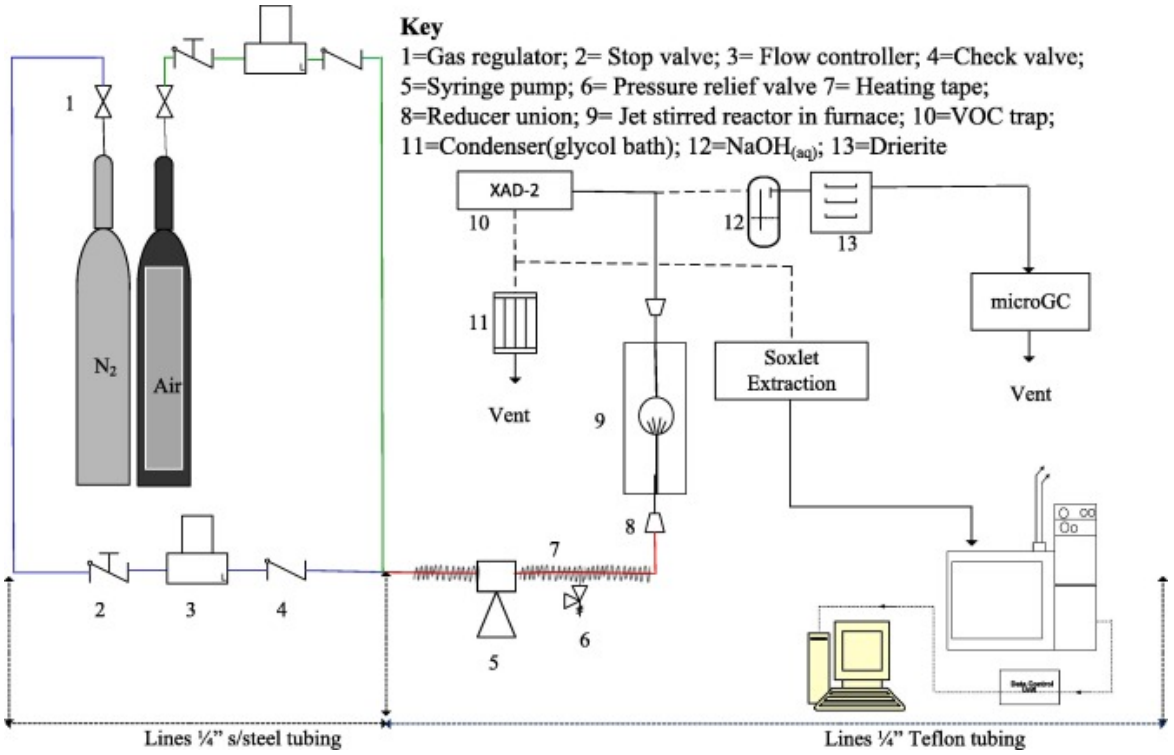

Fig. 2. Conversion of 1,3-D and percentage yields (× 1000) of mono- and di-chlorinated benzenes from thermal decomposition of 1,3-D, as a function of temperature. Quantified results are provided in Table S4.

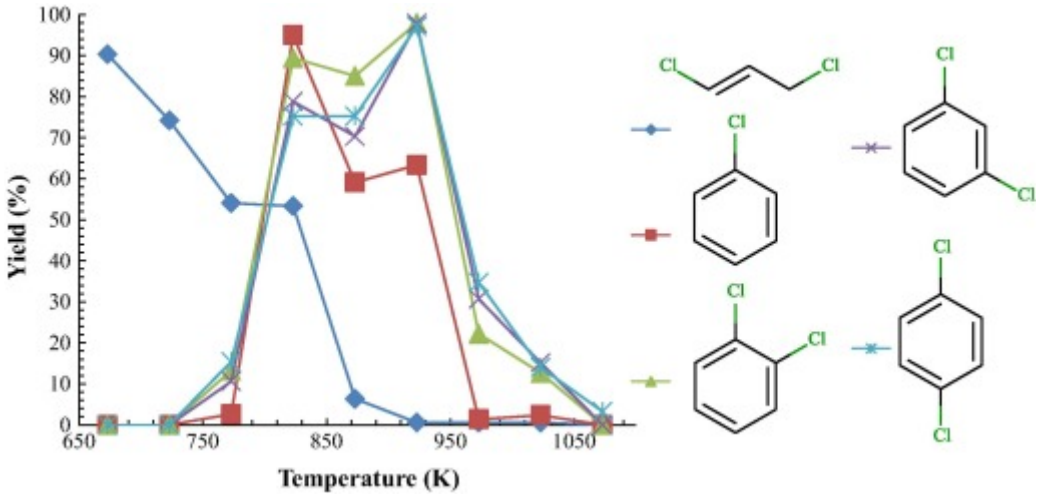

Fig. 3. Conversion of 1,3-D and percentage yields (× 1000) of tri-, tetra-, penta- and hexa-chlorinated benzenes from thermal decomposition of 1,3-D, as a function of temperature.

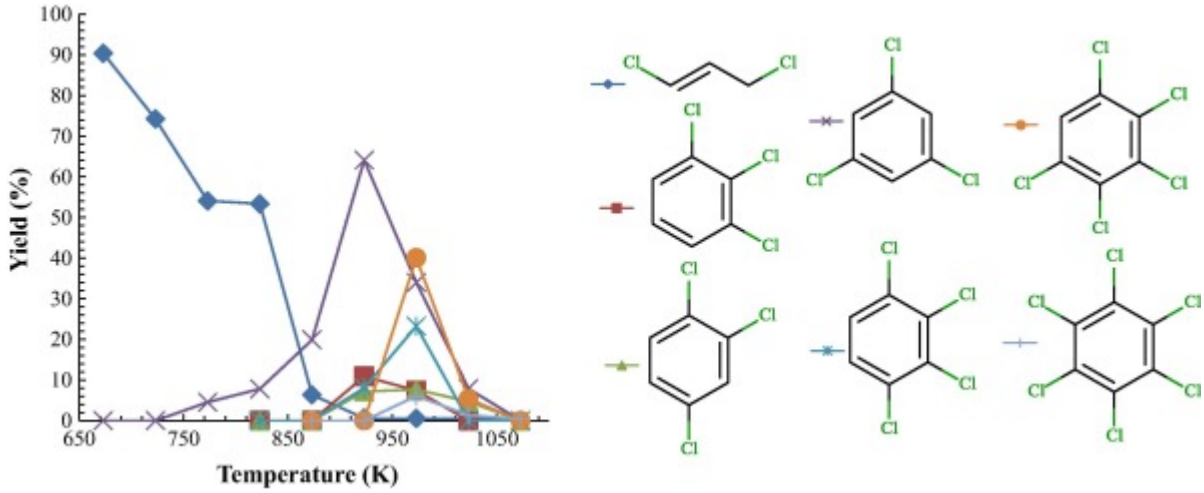

Fig. 4. Cyclisation pathway for conversion of 1,6-dichlorohexatriene radical (IM5) to chlorobenzene (P1). All values are given in kJ/mol, and include zero-point energy and thermal contributions at 298.15 K. G3MP2B3 results (top), M06-2X results (bottom).

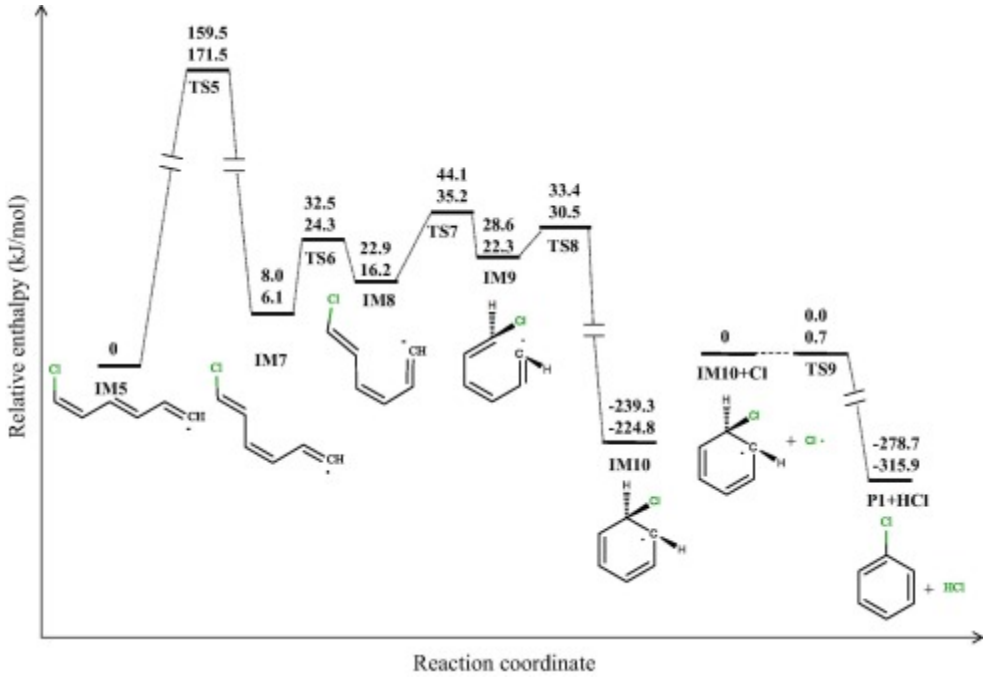

Fig. 5. Cyclisation pathway for 1,6-dichlorohexatriene radical (IM6) to IM14. All values are given in kJ/mol and include zero-point energy and thermal contributions at 298.15 K. G3MP2B3 results (top), M06-2X results (bottom).

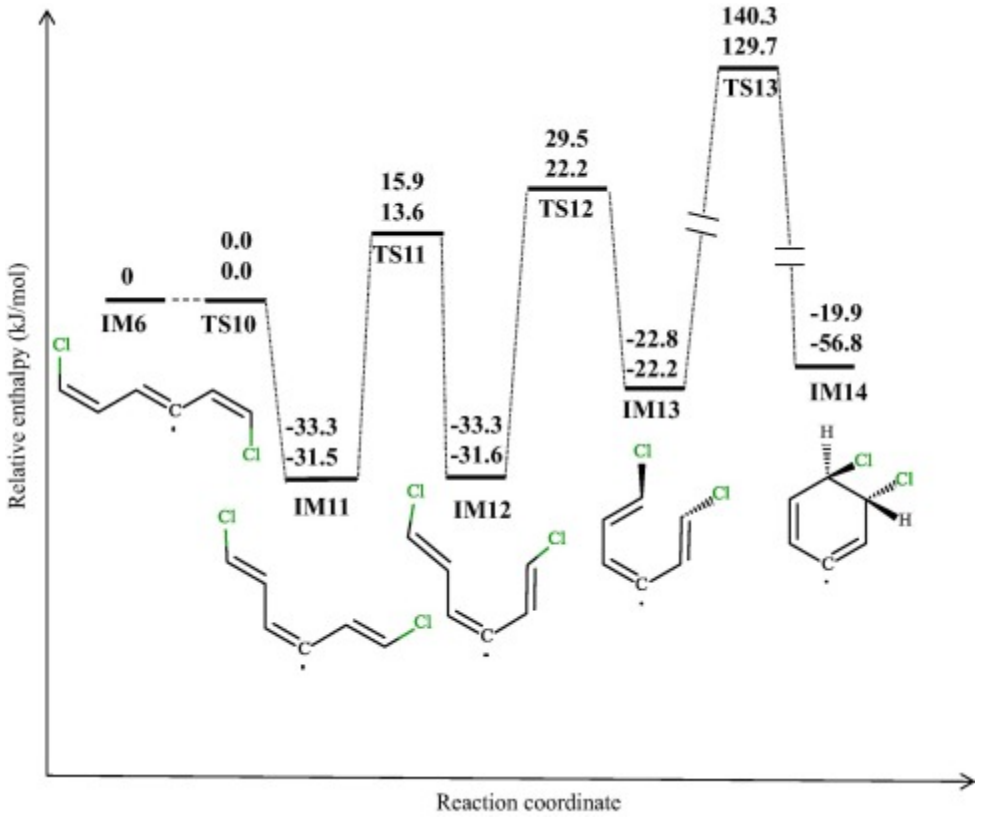

Fig. 6. Formation of chlorobenzene from IM14. All values are given in kJ/mol and include zero-point energy and thermal contributions at 298.15 K. G3MP2B3 results (top), M06-2X results (bottom).

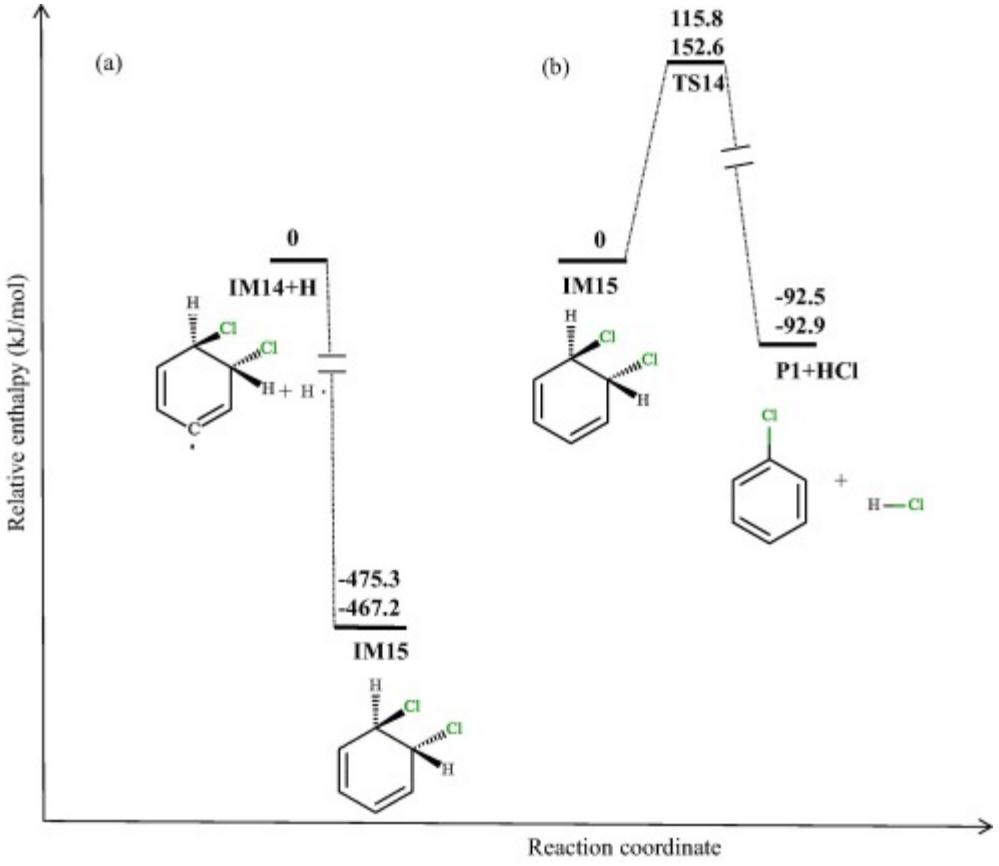

Scheme 1. $\Delta_r H^o_{298}$ (kJ/mol) for recombination of allylic radicals to form IM2 (a) and hydrogen abstraction by Cl radicals to form IM3 (b) and IM4 (c). G3MP2B3 results (top), M06-2X results (bottom).

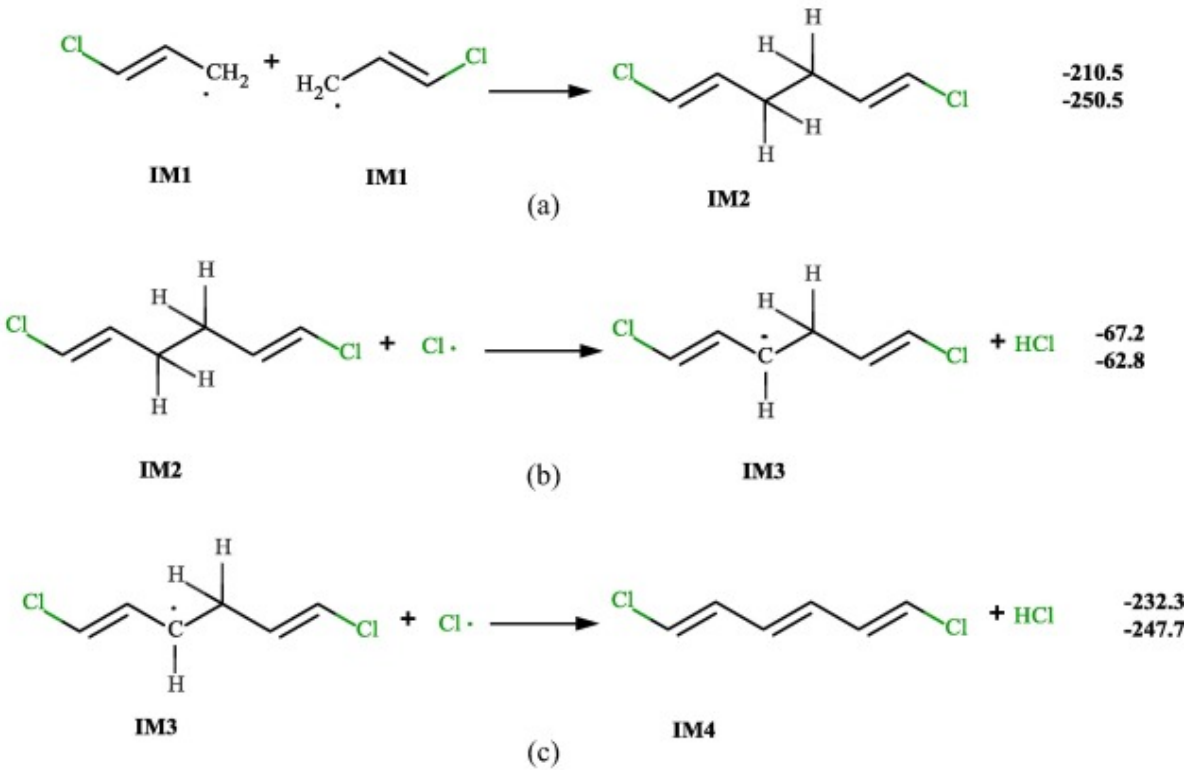

Scheme 2. $\Delta_r H^o_{298}$ (kJ/mol) for Cl/H abstraction by ambient Cl and H, G3MP2B3 results (top), M06-2X results (bottom).